electronics

Article

Carbon-Aware Demand Response for Residential Smart Buildings

Jiamin Zou [1], Sha Liu [1], Luxia Ouyang [1], Jiaqi Ruan [2] and Shuoning Tang [3,*]

[1] School of Architecture and Civil Engineering, Jinggangshan University, Ji'an 343009, China; zoujiamin@jgsu.edu.cn (J.Z.)
[2] College of Electrical Engineering, Sichuan University, Chengdu 610065, China
[3] College of Architecture and Urban Planning, Tongji University, Shanghai 200092, China
* Correspondence: tangshuoning@tongji.edu.cn

Abstract: The stability and reliability of a smart grid are challenged by the inherent intermittency and unpredictability of renewable energy as its integration into the smart grid increases. This places enormous pressure on the smart grid to manage high loads and volatility. To effectively mitigate the impact of new energy integration on smart grids, demand response (DR) can be altered to the demand-side burdens. Using residential smart buildings (RSBs) in Shanghai, this study proposes a carbon-aware demand response (CADR) model that is predicated on the coordination of power carbon intensity and real-time electricity prices. In order to accomplish a more comprehensive reduction in overall electricity consumption costs, we conducted real-time scheduling of a building's electrical devices using a greedy algorithm. In addition, a model of an optimal charging and discharging scheme for household electric vehicles was established, which is based on various charging modes, taking into account the electrification of the transportation sector. The cost of EV charging is reduced by an average of 23.18% and 33.2% under the two common charging modes, while the integrated cost of the total annual electricity consumption of household devices is reduced by 8.69%, as indicated by the simulation results.

Keywords: carbon-aware demand response; residential smart building; electric vehicle; smart grid

check for updates

Citation: Zou, J.; Liu, S.; Ouyang, L.; Ruan, J.; Tang, S. Carbon-Aware Demand Response for Residential Smart Buildings. *Electronics* **2024**, *13*, 4941. https://doi.org/10.3390/electronics13244941

Academic Editor: François Auger

Received: 12 November 2024
Revised: 8 December 2024
Accepted: 9 December 2024
Published: 14 December 2024

Copyright: © 2024 by the authors. Licensee MDPI, Basel, Switzerland. This article is an open access article distributed under the terms and conditions of the Creative Commons Attribution (CC BY) license (https://creativecommons.org/licenses/by/4.0/).

1. Introduction

A report by the International Energy Agency (IEA) indicates that electricity consumption in buildings accounts for 51.68% of the total electricity consumption in society [1]. The same report states that in 2022, electricity consumption accounted for 35% of energy consumption in buildings, and this rate is expected to rise to 48% by 2030 and to 70% by 2050. The trend of electrification in building energy consumption is significant, which undoubtedly poses great challenges for the smart grid in terms of high load management. To meet this challenge, a large number of demand-side management methods have been developed to manage demand-side resources, with demand response (DR) being an important method of demand-side management.

An important characteristic of a power system is that, at any given moment, the total generation capacity must match the total power load. Electricity prices are determined by a combination of factors, including supply and demand, electricity costs, and market structure. In traditional DR programs, independent system operators (ISOs) implement real-time pricing strategies, based on the locational marginal pricing (LMP) theory, to set electricity prices [2]. This method encourages electricity consumers to use power during periods of lower prices, shifting the power load from peak to off-peak periods by adjusting consumers' behavior, thereby optimizing the supply–demand balance and operational costs of the power system.

As the anticipation of a zero-carbon future grows and the energy transition advances, smart grids are gradually moving towards decarbonization [3]. Many thermal power units are being phased out, while the proportion of renewable energy sources, such as solar, wind, and hydro, is steadily increasing. Renewable energy generation does not rely on fossil fuels and can directly reduce carbon emissions from electricity. However, the power output from renewable energy is affected by weather and seasonal changes, requiring the grid to adapt to rapidly changing power supplies, which increases the complexity of grid dispatch and exacerbates the volatility of electricity prices [4,5]. The uncertainty in renewable energy supply also leads to increased volatility in carbon emissions from electricity. The intensified volatility poses challenges to traditional demand-side management, and under the drive towards zero-carbon goals, carbon awareness will play an increasingly significant role in demand-side management.

Many researchers have modeled and simulated smart grid systems, e.g., through demand-side and supply-side control and through the simulation of flexible load potentials in buildings. The objects of such a study include air conditioning units, lamps and lanterns, and smart home devices (e.g., washing machines and dishwashers) [6–10]. DR has been demonstrated to be an effective method for demand-side management. Furthermore, DR research emphasizes the importance of occupants' utilization behavior as a demand flexibility factor. The behavior of individuals within the building is considered in demand response, and certain users are also engaged in the development of DR programs in a variety of configurations [7,11–13]. The research on DR strategies that integrate hybrid energy application technologies is progressively increasing as the proportion of renewable energy applications in buildings continues to increase [14,15].

Due to advancements in digital and sensing technologies, future DR development is becoming increasingly oriented towards automated demand response (DR). Advanced metering infrastructure (AMI) devices are a reliable two-way communication system that can establish connections between consumers and the power sector. In a smart grid, smart appliances can effectively utilize time-varying rates and dynamic rates to reduce costs [16–25]. Currently, many optimization algorithms are used for automated DR strategies, such as linear programming (LP) methods [16,17], genetic algorithms (GAs) [18,19], model predictive control (MPC) [12,20,21], and machine learning methods [22–25]. Although previous studies have provided an overview of DR measures, several research gaps have not been sufficiently addressed in the current research.

Firstly, traditional energy management focuses solely on electricity prices without considering the dynamic changes in system carbon emission intensity, making it difficult to maximize the economic and emission reduction benefits that energy management can bring [26,27]. Therefore, going beyond traditional energy management models and designing suitable electricity–carbon coordinated demand-side management schemes will be more applicable to a zero-carbon future and for promoting energy transition.

Secondly, dynamic pricing strategies based on demand response have been thoroughly researched and applied. In previous studies, some users have participated in demand response programs in various forms [28,29]. However, since each user's equipment exhibits unique behavior, residential equipment varies significantly across different studies, making it difficult to compare and evaluate research results with other studies.

Thirdly, there has been an explosive growth in the use of electric vehicles in emerging markets and developing economies (China, India, and Indonesia), with over 50 countries, accounting for about 60% of the world's population, having implemented policies to incentivize their use [1]. Electric vehicles are set to become an important part of household electrical equipment, but there is a lack of sufficient research in this area in the existing literature.

Using intelligent control and data analysis systems, users can automatically control electrical devices, thereby attaining automated DR by collecting energy consumption data inside buildings. This capability is enabled by the advancement of IoT technology in buildings [4,5]. The optimization model is the central hub of automated disaster recovery,

responsible for scheduling a variety of devices to reconcile varying interests. This study develops a scheduling optimization model that is tailored to the power market for typical electrical devices in residential smart buildings (RSBs). It employs a greedy algorithm to approximate the optimal scheduling of residential building electrical devices and achieve carbon-aware DR (CADR). The primary contributions of this study to the existing literature are as follows:

1. A power–carbon collaborative DR strategy for domestic devices is proposed, which is based on traditional DR. The dynamic changes in carbon emission intensity are also incorporated into DR, which reduces electricity costs for household consumers and decreases power-related carbon emissions. This strategy also takes into account the time-varying character of prices.
2. In order to improve the model's universality, a scheduling optimization model is developed using typical domestic devices. The model incorporates an electric vehicle charging mode to investigate the optimal power scheduling scheme under various household charging modes, as the electrification of the transportation industry (i.e., the rapid growth of electric vehicles) has altered the pattern of traditional power loads.

The rest of the paper is organized as follows: the typical electrical device and usage characteristics in RSBs is described in Section 2. A mathematical model of CADR is developed in Section 3. Case studies and simulation results are discussed in Section 4. Finally, the main conclusions are provided in Section 5.

2. Typical Electrical Device and Usage Characteristics in RSBs

2.1. Types and Power of Typical Electrical Device in RSBs

Typical electrical devices in RSBs are electrical devices that are commonly owned and used by families in a certain area. This study defined the types and quantities of typical devices in RSBs based on the relevant statistical data from the National Bureau of Statistics of China and established an average household equipment model for urban households in Shanghai [30]. As can be seen from the data in Table 1, nearly half of the households in Shanghai own a car, with about 20% being electric vehicles. Washing machines, refrigerators, water heaters, microwave ovens, range hoods, and computers are prevalent in most households. In addition to the aforementioned durable consumer goods, household lighting equipment, dryers, and rice cookers (a traditional Chinese kitchen device) are also typical electrical devices.

Table 1. Ownership of major electrical devices in residential buildings in Shanghai [30].

Main Types of Durable Consumer Goods	Vehicle	Washing Machine	Refrigerator	Microwave Oven	Television	Air Conditioner	Water Heater	Hood	PC
Average ownership per 100 urban households	45.4	97.3	103.3	85.7	174.2	216	100.4	87.2	105.0

The benchmark power for typical household appliances was determined using the mode method, which selects the most commonly used rated power within the most popular price range for household appliances available on the market as the benchmark strategy for that category of appliances. The data for the rated power were sourced from JD.com®, one of China's largest online shopping platforms. The statistical results are shown in Table 2.

Table 2. Common power of residential building devices.

Type of Device	Price Range (CNY)	Power
Refrigerator	1714–4014	780 w/24 h
Television	2636–4938	220 w/h
Computer	4680–7512	200 w/h
Hood	973–3248	300 w/h
Rice cooker	284–492	750 w/h
Microwave oven	492–678	1000 w/h
Water heater	500–1000	2500 w/h
Washing machine	1207–3378	500 w/h
Dryer		1000 w/h

2.2. Schedule of Typical Electrical Devices in RSBs

For typical electrical devices, usually only the schedules and loads for lighting and air conditioning can be found in the building energy standards of various countries. However, considering that the operation schedule of household electrical devices is closely related to household activities, this article summarizes the typical household routines based on the schedules for lighting, air conditioning, and occupancy rates in building energy standards. Based on this, we derived the operation schedules for typical household electrical appliances. The case study for this research is Shanghai, China, and therefore, the Chinese building energy standards are used as the schedule and load standards [31]. The specific schedules for lighting, air conditioning, and occupancy rates are shown in Figure 1.

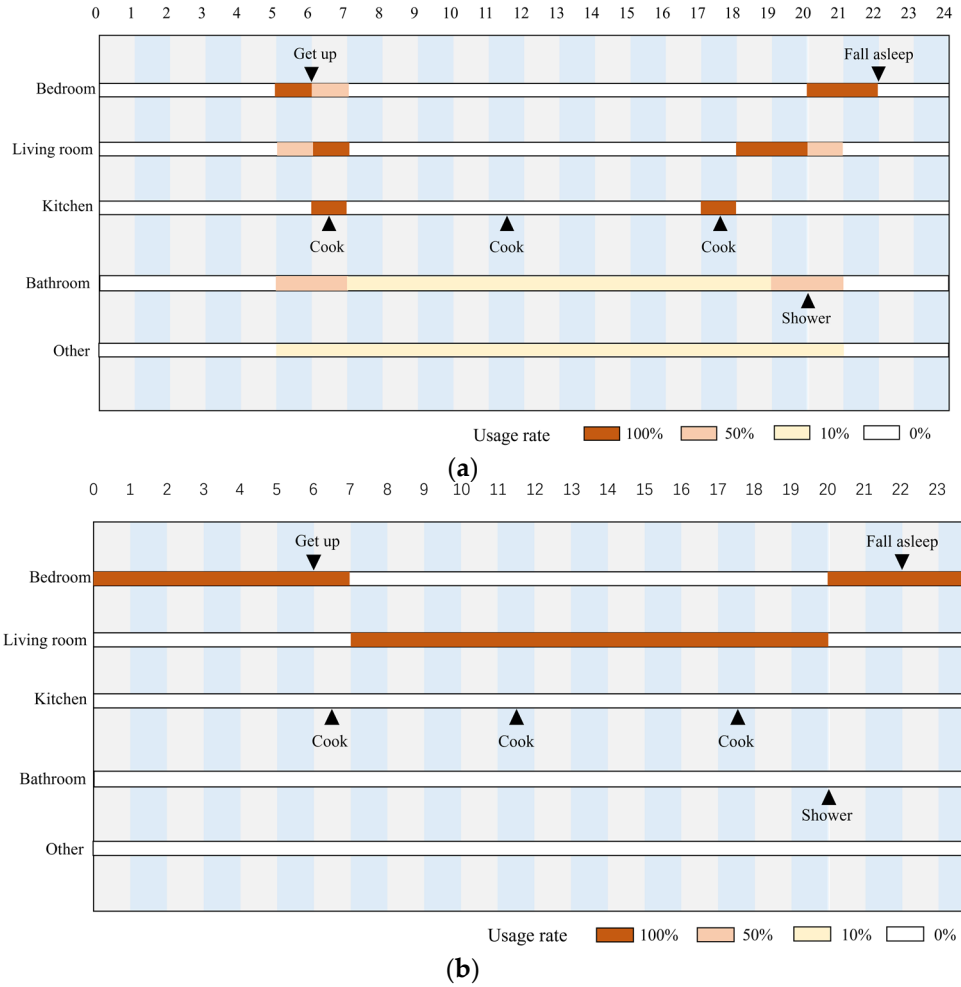
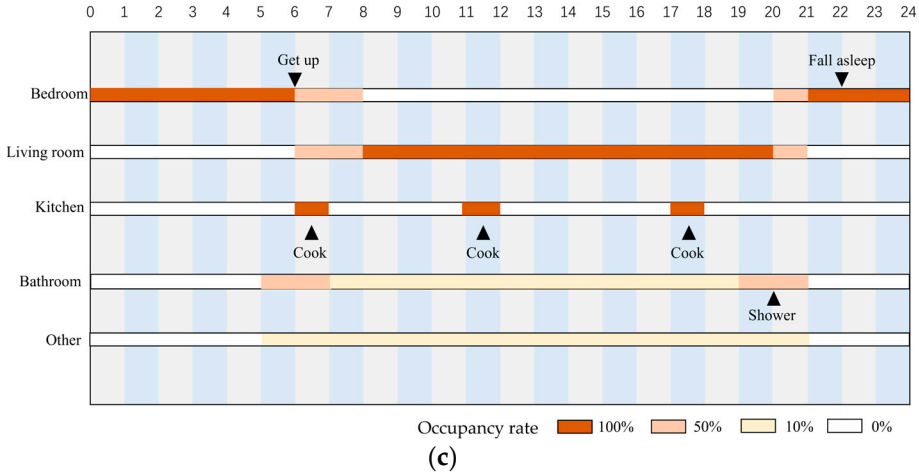


Figure 1. *Cont.*



(**c**)

Figure 1. (**a**) Lighting schedule for all days; (**b**) air conditioning schedule for all days; and (**c**) room occupancy rate for all days.

Based on the timetable depicted in Figure 1, it is evident that the work and rest hours of a typical Shanghai family are as follows: waking up and preparing breakfast at 6–7 a.m., cooking lunch at 11–12 a.m., cooking dinner at 5–6 p.m., washing up at 8–9 p.m., and retiring to bed at approximately 10 p.m. The activities of individuals in their bedrooms are primarily concentrated during the wake-up period and the first 1–2 h before bed, while the activities of those in the home after waking up and before bedtime are primarily conducted in the living room. The bathroom is frequently used after waking up and before going to bed, and the kitchen is used during cooking times. This schedule applies to every day.

According to the schedule, we summarized the usage times and rates of different appliances. Except for the refrigerator, which operates continuously for 24 h, the TV and PC, as entertainment appliances, may be used from the time of waking up to before going to sleep. The use of the water heater, washing machine, and dryer is associated with bathing activities. The water heater starts running one hour before bathing, while the washing machine and dryer are used after bathing. The range hood, rice cooker, and microwave, as kitchen appliances, are used alternately during cooking times (Figure 2).

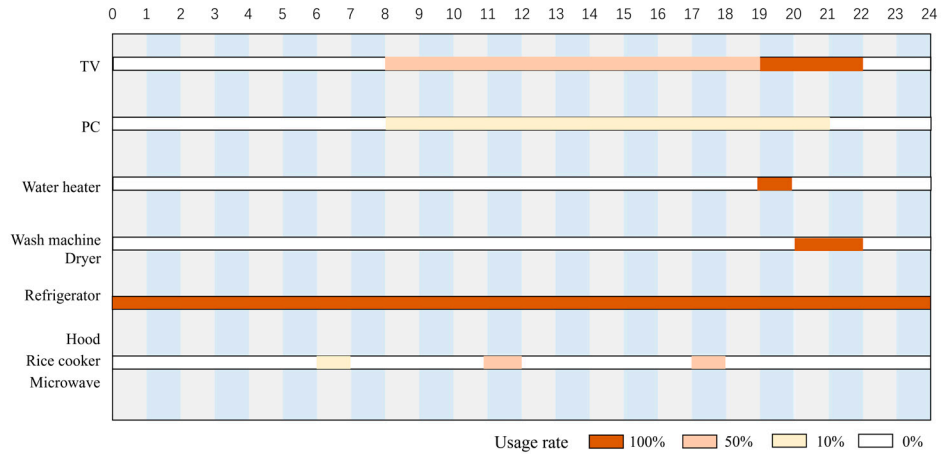


Figure 2. Device schedule for all days.

3. Dispatchable Optimization Model for Typical Electrical Devices in RSBs

3.1. Method

The objective of this study is to minimize the electricity costs and carbon emissions of buildings by transferring transferable loads, while maintaining the total electricity consumption of typical electrical devices in RSBs. Except for the washing machine and dryer, almost all typical electrical devices operate independently. Consequently, each device can be optimized for load transfer independently, resulting in a collective optimization model for typical electrical devices. This study implements a greedy algorithm to optimize the transmission of devices across the entire collection in accordance with these traits. Greedy algorithms are often used to solve NP-hard problems. However, there is no universal greedy solution that applies to all NP-hard problems. In fact, different greedy algorithms can be proposed based on the nature of the optimization problem. Greedy algorithms are particularly suitable for the optimization problems presented in this paper, as they provide the best possible scheduling for the given devices.

The specific process is as follows: a greedy algorithm is used to incrementally optimize the scheduling of each appliance, thereby obtaining the optimal scheduling plan for each device, which is a local optimal solution. Then, the optimal solutions for all devices are summed to achieve the minimum comprehensive cost of electricity and carbon emissions for the day. To comprehensively assess the sensitivity of the model, optimization simulations were conducted for each day of the year based on the hourly electricity rates and carbon emission data for the entire year of 2023.

3.2. Optimization Model

In RSB electrical loads, there are flexible loads and rigid loads. Flexible loads participate in the grid's collaboration as controllable resources without affecting users' normal activities. In typical household appliances, the electricity consumption of lighting, air conditioning, refrigerators, range hoods, microwaves, computers, and televisions is considered the base load, which means these devices operate stably during the required time and have no transferable or interruptible characteristics. Electric rice cookers, water heaters, washing machines, dryers, and electric vehicles are considered to have transferable loads. Among them, the electricity usage of electric rice cookers, water heaters, washing machines, and dryers is transferable but not interruptible, while the electricity usage of electric vehicles is both interruptible and transferable.

The base load expression for RSB electrical devices is as follows:

$$E_{base} = E_{lighting} + E_{air} + E_{tv} + E_{\text{refrigerator}} + E_{pc} + E_{hood} + E_{microwave} \quad (1)$$

The transferable load expression is as follows:

$$E_{trans} = E_{wash} + E_{dryer} + E_{waterheater} + E_{rice} + E_{car} \quad (2)$$

The sum of the base load and transferable load is the total building electricity consumption.

$$E_{building} = E_{base} + E_{trans} \quad (3)$$

The daily electricity cost for RSBs is calculated as follows:

$$PC_{building} = PC_d^{trans} + PC_d^{base} \quad (4)$$

$$PC_d^{trans} = \sum_{h=1}^{24} E_{trans,h} \times P_h \quad (5)$$

$$PC_d^{base} = \sum_{h=1}^{24} E_{base,h} \times P_h \quad (6)$$

The daily carbon emission cost of electricity for RSBs is calculated as follows:

$$CC_{building} = CC_d^{trans} + CC_d^{base} \tag{7}$$

$$CC_d^{trans} = \sum_{h=1}^{24} E_{trans,h} \times C_h \tag{8}$$

$$CC_d^{base} = \sum_{h=1}^{24} E_{base,h} \times C_h \tag{9}$$

The daily comprehensive cost of electricity for RSBs is calculated as follows:

$$TC_{building} = PC_{building} + CC_{building} \tag{10}$$

where $PC_{building}$ is the annual electricity cost of a building. PC_d^{trans} represents the daily electricity cost of the building's transferable load. PC_d^{base} is the daily electricity cost of the building's transferable load. $CC_{building}$ is the annual carbon cost of the building. CC_d^{trans} is the daily carbon cost of the building's transferable load. PC_d^{base} is the daily carbon emission cost of the building's transferable load. P_h is the electricity price at the moment h. C_h is the carbon emission cost at the moment h. $TC_{building}$ is the comprehensive cost of the building.

The objective of optimization is to minimize the building's yearly electricity cost and carbon emissions by optimizing the transfer of transferable loads in accordance with the hourly dynamic electricity price and dynamic carbon emission. This is achieved while ensuring that the total electricity consumption of each device remains constant. The optimization model employs the greedy algorithm to optimize the transferable loads for each day of the year to determine the minimum value of electricity cost and carbon emission cost for each day, which is the local optimal solution (Figure 3). The optimal solutions for each day are then added together to determine the minimum electricity cost and carbon emission cost for the entire year.

$$minPC_{i,d} = \sum_{t=1}^{24} E_{i,h}^{trans} \times P_h \tag{11}$$

$$minCC_{i,d} = \sum_{t=1}^{24} E_{i,h}^{trans} \times C_h \tag{12}$$

where $minPC_{i,d}$ is the minimum daily cost of electricity after the transfer of the ith device; $E_{i,h}^{trans}$ is the electricity consumption at the moment h after the transfer of the ith device; and $minCC_{i,d}$ is the minimum daily cost of carbon emission after the transfer of the ith device.

The minimum total cost of each transferable electrical device is summed to obtain the daily minimum electricity cost and carbon emission cost of all transferable devices.

$$minPC_d^{trans} = \sum_{i=1}^{5} min\ PC_{i,d} \tag{13}$$

$$minCC_d^{trans} = \sum_{i=1}^{5} min\ CC_{i,d} \tag{14}$$

The minimum daily comprehensive cost of RSBs is calculated as follows:

$$minTC_{building} = minPC_{building} + minCC_{building} \tag{15}$$

$$minPC_{building} = minPC_d^{trans} + PC_d^{base} \tag{16}$$

$$minCC_{building} = minCC_d^{trans} + CC_d^{base} \tag{17}$$

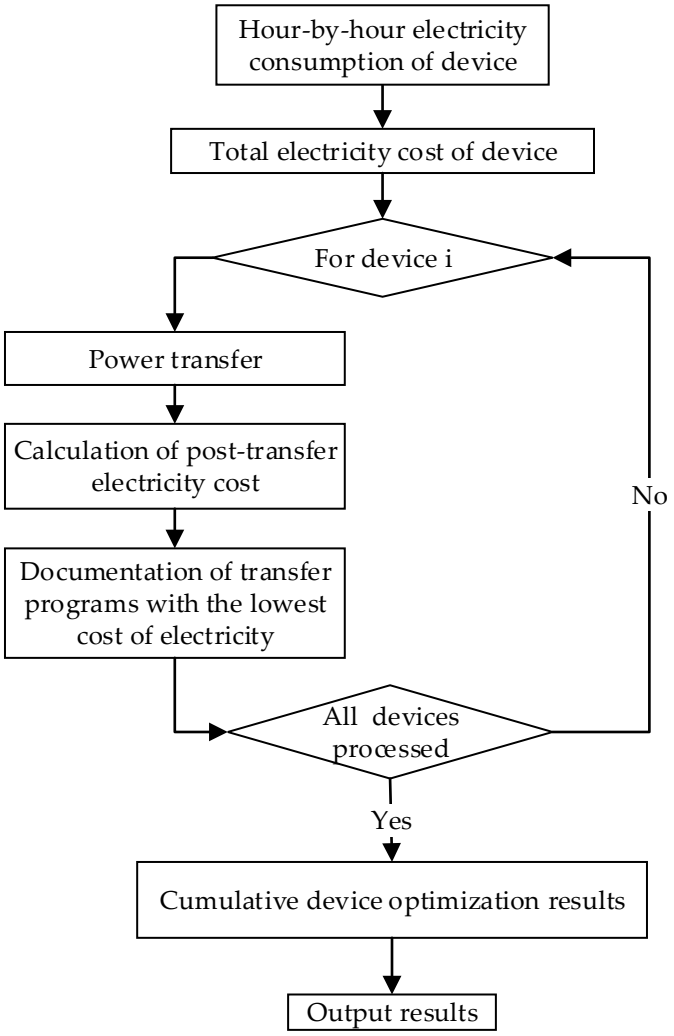


Figure 3. Optimization processes.

3.3. Typical Electrical Device Load Transfer Optimization Models

Rice cookers, water heaters, washing machines, and dryers are four types of equipment whose operating times can be shifted within a certain range, but once started, they must run continuously until the work is completed. The constraints on their shift range are closely related to household behavior.

3.3.1. Rice Cooker

The rice cooker is utilized more than once per day, and its load interval can only be advanced from the preparation time and cannot be earlier than the most recent use time. The rice cooker can be utilized only once during the lunch and dinner hours, as the load periods for these meals can be combined. It is understood that the rice cooker is utilized three times per day, and its moments are represented by the symbols x, y, and z.

$$PC_{rice} = E_{wash}\ (x)\ \times\ P_x + E_{wash}\ (y)\ \times\ P_y + E_{wash}\ (z)\ \times\ P_z \tag{18}$$

To minimize PC_{rice}, it is necessary to find the minimum comprehensive cost for each interval. The moment h_x with the lowest cost in the interval $[1, x]$ is as follows:

$$h_x = \arg min_{t\in[1,x]} PC_{rice}\ (h) \tag{19}$$

The moment $h_{x\to y}$ with the lowest cost in the interval $[x+1, y]$ is as follows:

$$h_{x\to y} = \arg min_{t\in[x+1,y]} PC_{rice}\ (h) \tag{20}$$

The moment $h_{y\to z}$ with the lowest cost in the interval $[y+1, z]$ is as follows:

$$h_{y\to z} = \arg min_{t\in[y+1,z]} PC_{rice}\ (h) \tag{21}$$

Based on the comparison of the costs of $h_{x\to y}$ and $h_{y\to z}$, a decision is made on how the electricity will be transferred.

If

$$PC_{rice}\ \left(h_{x\to y}\right)\ <\ PC_{rice}\ \left(h_{y\to z}\right) \tag{22}$$

then

$$E_{new}\left(h_{x\to y}\right) = \sum_{h=x+1}^{y} E_{rice}\ (h) \tag{23}$$

If not,

$$E_{new}\left(h_{x\to y}\right) = E_{rice}\ (y) E_{rice}\ \left(h_{y\to z}\right) = \sum_{h=y+1}^{z} E_{rice}\ (h) \tag{24}$$

The cost after optimizing the transfer is

$$min\ PC_{rice} = E_{new,x}\ \times\ P_{h_x} + E_{new,y}\ \times\ P_{h_{x\to y}} + E_{new,z}\ \times\ P_{h_{y\to z}} \tag{25}$$

3.3.2. Washing Machine and Dryer

The washing machine can be rescheduled from its initial time of use, and the majority of washing machines now have a 24 h reservation feature. This allows the washing machine to be operated at the least expensive time of day, while the dryer must be operated immediately following the washing machine. The transfer optimization model for the washing machine and dryer is as follows:

$$min\ PC_{total} = min\Big(E_{wash}\ \times\ P_h +\ E_{dryer}\ \times\ P_{h+1}\Big) \tag{26}$$

3.3.3. Water Heater

The water heater is exclusively intended for forward transfer from the laundry process, and the transfer interval must not exceed two hours to prevent the consumption of additional power for reheating. The water heater's transmission optimization model is as follows:

$$PC_{waterheater} = \sum_{h=1}^{24} E_{waterheater,h} \times P_h \tag{27}$$

$$min\ PC_{waterheater} = \sum_{h=1}^{24} PC_h \tag{28}$$

$$PC_h = \Big(\ E_h - \sum_{k=0}^{2} E_{h-k}\ \times\ 1_{\{d_{h-k}=k\}}\Big)\ \times\ P_h \tag{29}$$

The transfer time limit is as follows: for all h, d_h can be designated as 0, 1, or 2.

Non-negative power consumption: for all h, the power consumption after the transfer is as follows:

$$E_h - \sum_{k=0}^{2} E_{h-k}\ \times\ 1_{\{d_{h-k}=k\}}\ \geq 0 \tag{30}$$

3.3.4. Electric Vehicle (EV)

In China, EV consumers are allowed to install charging posts in their parking spaces in residential neighborhoods. The common models of home charging posts are 7 kW and 11 kW, and the main charging time for most home EV owners is between dinner and breakfast, i.e., from 7:00 p.m. to 7:00 a.m. the next morning.

According to a government report, by 2025, the range of new entirely electric passenger cars should reach 12 kWh/100 km [32]. Combined with the average 15% mileage difference in the ICCT report [33], this study adopted 13.8 kWh/100 km as the baseline energy consumption of EVs. The ICCT report also pointed out that pointed out that some household EV owners have a certain degree of mileage anxiety, and about 50% of charging occurs when the battery power is more than 50%. According to the data from an industry report [34], in 2022, the average annual mileage of Chinese cars was 15,400 km, and the annual electricity consumption was 2152.2 kWh.

Based on different charging behaviors, two charging modes are summarized (Table 3). Mode 1 assumes charging begins when the battery reaches a deep discharging state (below 10% remaining) until it is fully charged. Mode 2 assumes a fixed weekly charging schedule when the battery is in a partial discharge state. Taking an electric vehicle with a battery capacity of approximately 77 kW as an example, using Mode 1 requires charging 28 times a year (13 date combinations annually), with a 7 kW charging station requiring 11 h per charge, and an 11 kW charging station requiring 7 h per charge. Using Mode 2 requires charging 52 times a year (seven date combinations annually), with a 7 kW charging station requiring 6 h per charge, and an 11 kW charging station requiring 4 h per charge. For both modes, the charging period is from 7:00 p.m. to 7:00 a.m. the next day. Since electric vehicle charging is an interruptible load, charging can be paused if electricity prices suddenly rise and resumed when prices return to a reasonable range.

Table 3. Common power of residential building devices.

Mode	Battery Status During Charging	Charging Frequency	Annual Charging Frequency	Charging Date Combinations
1	Deep discharging (≤10)	Charge every 11 days	28	13
2	Partial discharge (≥50%)	Charge every 7 days	52	8

The charging date for Charging Mode 1 is

$$DATE_{\alpha} = \{D_{\alpha} + (i-1) \times 12 \mid i = 1, 2, \cdots, 28\} \tag{31}$$

$$D_{\alpha} = \{1, 2, \cdots, 13\} \tag{32}$$

The date following the charging day is expressed as follows:

$$DATE'_{\alpha} = DATE_{\alpha} + 1 \tag{33}$$

The charging date for Charging Mode 2 is

$$DATE_{\beta} = \{D_{\beta} + (i-1) \times 7 \mid i = 1, 2, \cdots, 52\} \tag{34}$$

$$D_{\beta} = \{1, 2, \cdots, 8\} \tag{35}$$

The date of the day following the charging day is

$$DATE'_{\beta} = DATE_{\beta} + 1 \tag{36}$$

Before transfer optimization, each charge is continuous, and the cost of 7 kW of charging station electricity in the case of Charging Mode 1 is

$$PC_{DATE_{\alpha}} = E_{7kW} \times \sum_{h=19}^{24} P_{DATE_{\alpha,h}} + E_{7kW} \times \sum_{h=1}^{5} P_{DATE'_{\alpha,h}} \tag{37}$$

The cost of 11 kW of charging station electricity in the case of Charging Mode 1 is

$$PC_{DATE_{\alpha}} = E_{11kW} \times \sum_{h=19}^{24} P_{DATE_{\alpha,h}} + E_{11kW}11 \times P_{DATE'_{\alpha,1}} \tag{38}$$

The cost of 7 kW of charging station electricity in the case of Charging Mode 2 is

$$PC_{DATE_\beta} = E_{7kW} \times \sum_{h=19}^{24} P_{DATE_{\beta,h}} \tag{39}$$

The cost of 11 kW of charging station electricity in the case of Charging Mode 2 is

$$PC_{DATE_\beta} = E_{11kW} \times \sum_{h=19}^{22} P_{DATE_{\beta,h}} \tag{40}$$

The cost optimization for EV charging is carried out by using interruptive charging and selecting a moment for charging, from 7:00 p.m. on the charging day to 7:00 a.m. on the following day. The comprehensive power cost series from 7:00 p.m. on the charging day to 7:00 a.m. the next day for Charging Mode 1 as follows:

$$P_{EV1} = \left\{ \begin{array}{c} P_{DATE_{\alpha,19}}, P_{DATE_{\alpha,20}}, P_{DATE_{\alpha,21}}, P_{DATE_{\alpha,22}}, P_{DATE_{\alpha,23}}, P_{DATE_{\alpha,24}}, \\ P_{DATE'_{\alpha,1}}, P_{DATE'_{\alpha,2}}, P_{DATE'_{\alpha,3}}, P_{DATE'_{\alpha,4}}, P_{DATE'_{\alpha,5}}, P_{DATE'_{\alpha,6}}, P_{DATE'_{\alpha,7}} \end{array} \right\} \tag{41}$$

The electricity rates are sorted from lowest to highest:

$$P'_{EV1} \rightarrow Sort\ (P_{EV1}) \tag{42}$$

The minimum power cost for a 7 kW charging station in the case of Charging Mode 1 is as follows:

$$min\ PC_{DATE_\alpha} = E_{7kW} \times \sum_{i=1}^{11} P'_{EV1,i} \tag{43}$$

The minimum power cost for an 11 kW charging station in the case of Charging Mode 1 is as follows:

$$min\ PC_{DATE_\alpha} = E_{11kW} \times \sum_{i=1}^{7} P'_{EV1,i} \tag{44}$$

The amount of a resident's electricity bill from 7:00 p.m. to 7:00 a.m. the following day under Charging Mode 2 is calculated as follows:

$$P_{EV2} = \left\{ \begin{array}{c} P_{DATE_{\beta,19}}, P_{DATE_{\beta,20}}, P_{DATE_{\beta,21}}, P_{DATE_{\beta,22}}, P_{DATE_{\beta,23}}, P_{DATE_{\beta,24}}, \\ P_{DATE'_{\beta,1}}, P_{DATE'_{\beta,2}}, P_{DATE'_{\beta,3}}, P_{DATE'_{\beta,4}}, P_{DATE'_{\beta,5}}, P_{DATE'_{\beta,6}}, P_{DATE'_{\beta,7}} \end{array} \right\} \tag{45}$$

The electricity rates are sorted from lowest to highest:

$$P'_{EV2} \rightarrow Sort\ (P_{EV2}) \tag{46}$$

The minimum power cost for a 7 kW charging station in the case of Charging Mode 2 is follows:

$$min\ PC_{DATE_\beta} = E_{7kW} \times \sum_{i=1}^{6} P'_{EV2,i} \tag{47}$$

The minimum power cost for an 11 kW charging station in the case of Charging Mode 2 is as follows:

$$min\ PC_{DATE_\beta} = E_{11kW} \times \sum_{i=1}^{4} P'_{EV2,i} \tag{48}$$

4. Simulation Results and Discussion

4.1. Case Study

The RSB in Shanghai used as a case study object in this paper is depicted in Figure 4. The standard floor of the building has a total area of 751.52 m^2, while a single-unit suite has a total area of 39.64 m^2. The story is 3 m high, and each story contains 14 households. The building has a total of six stories and 84 households.

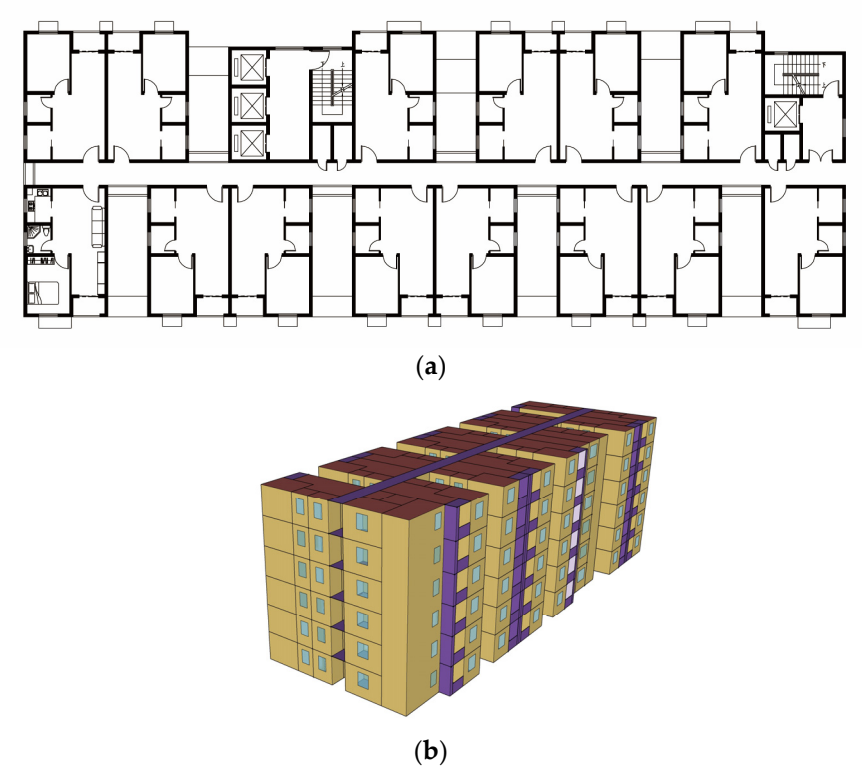


Figure 4. (**a**) Building plan and (**b**) building model.

According to the Shanghai Local Standard [35], residences with a household area of less than 90 m^2 should construct parking spaces with a ratio of 1:1 for the total number of households. A Shanghai government report estimates that the number of new energy vehicles in Shanghai would reach 1,288,000 in 2023 [36], which would account for 22.74% of the number of motor vehicles in Shanghai. In this case, the number of household EVs was allocated according to a rate of 20% of the number of households.

4.2. Simulation Results

Based on the power and usage schedule of appliances, the EnergyPlus software (Version 23.2.0) and 2023 meteorological data were used to simulate the electricity consumption of this residence. The hourly and daily electricity consumption of all appliances was obtained. Non-shiftable loads account for 75.12% of the annual electricity consumption, while shiftable loads account for 24.88%. On a daily basis, the proportion of shiftable loads to total daily electricity consumption fluctuates between 12.31% (9 January) and 30.86% (9 May). Changes in air conditioning load are the reason for this fluctuation, as there is a significant negative correlation between the proportion of air conditioning load and the proportion of shiftable loads (Figure 5).

The application of a greedy algorithm for the transfer optimization of transferable loads resulted in a 21.95% reduction in the comprehensive cost of annual transferable loads and an 8.69% reduction in the comprehensive cost of total annual electricity consumption (Figure 6). On a daily basis, the reduction in comprehensive electricity cost of transferable loads fluctuated between 2.08% (on 6 January) and 75.09% (on 18 June), with the daily comprehensive electricity cost reduced by more than 10% on 214 days throughout the year.

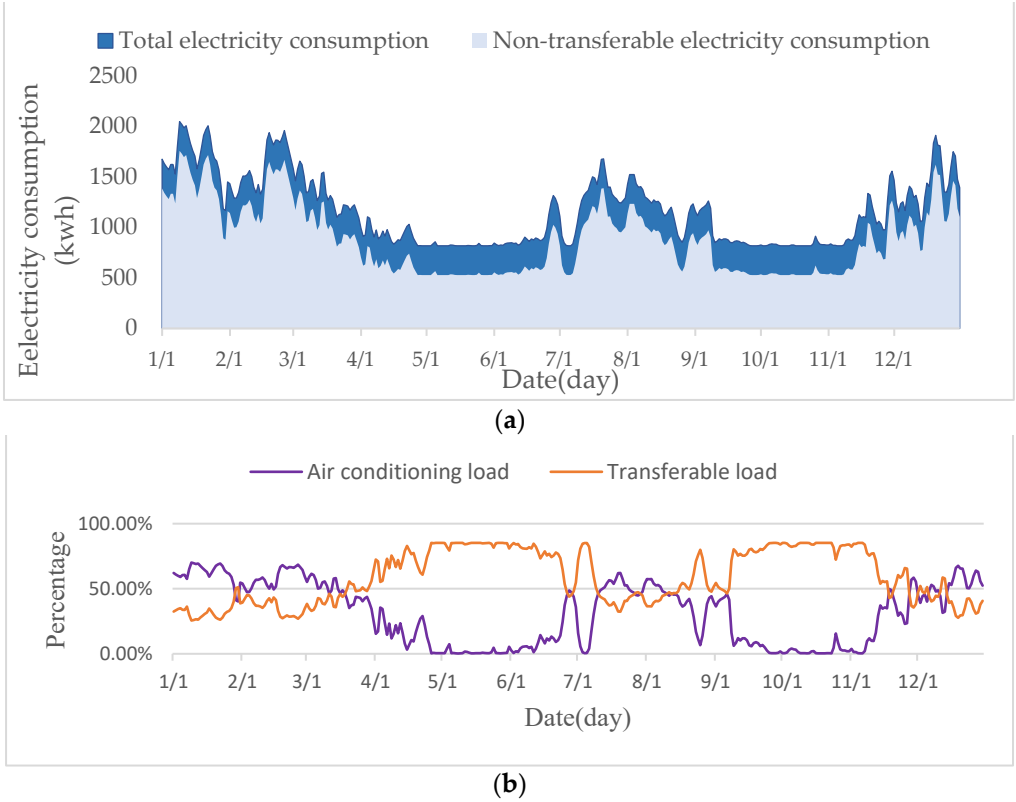


Figure 5. (**a**) Annual building electricity consumption and (**b**) air conditioning load and transferable load.

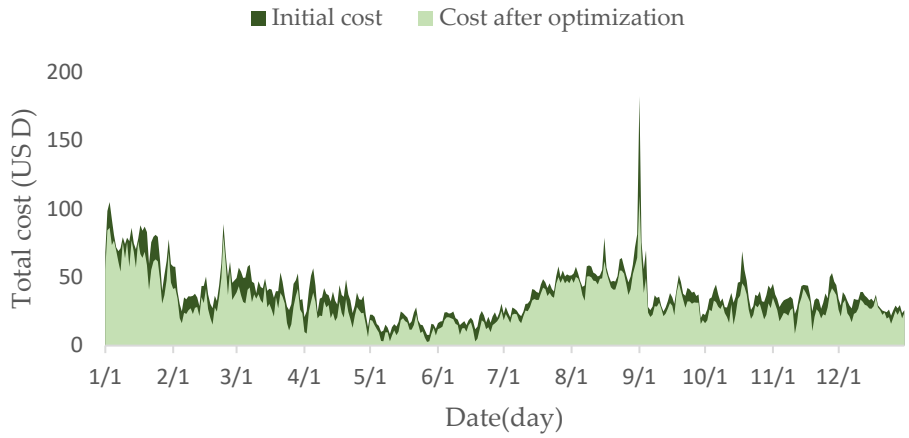
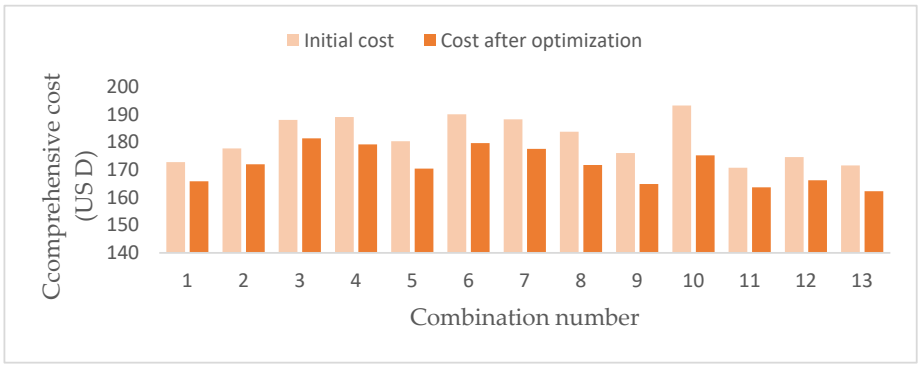


Figure 6. Optimization results for transferable loads.

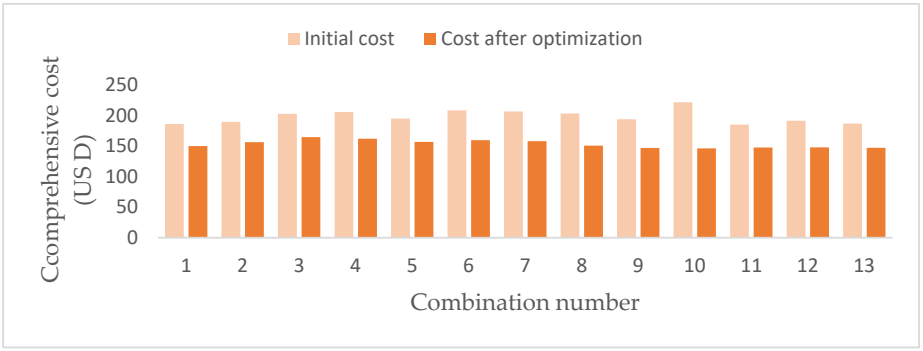
4.3. EV Transfer Optimization Results

The average comprehensive cost of a 7 kW charging station is USD 181.29 in Charging Mode 1, while the optimized average comprehensive cost is USD 171.58, resulting in an average reduction of 5.33%. On the other hand, the average comprehensive cost of an 11 kW charging station is USD 198.35, and the optimized average comprehensive cost is USD 153.43, resulting in an average reduction of 22.48% (Figure 7).

In Charging Mode 2, the average comprehensive cost of the 7 kW charging station is USD 204.49, and the optimized average comprehensive cost is USD 151.47, resulting in an average reduction of 25.62%. Similarly, the average comprehensive cost of the 11 kW charging station is USD 233.07, and the optimized average comprehensive cost is USD 154.62, reflecting an average reduction of 33.2% (Figure 8).

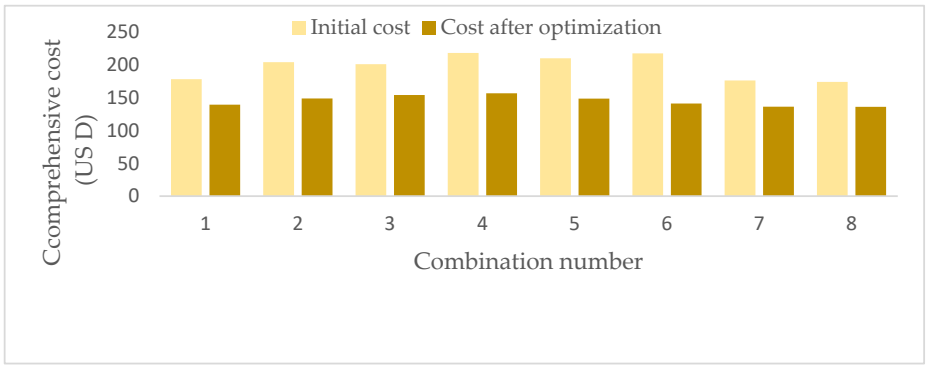


(**a**)

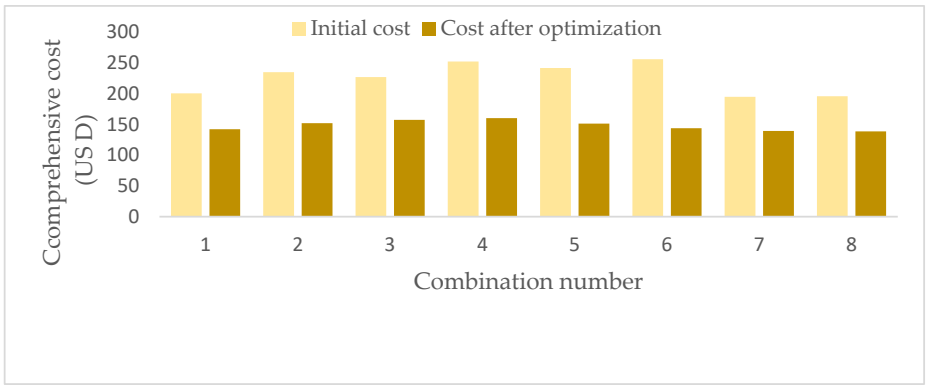


(**b**)

Figure 7. (**a**) Optimization results for 7 kW charging station under Charging Mode 1 and (**b**) optimization results for 11 kW charging station under Charging Mode 1.



(**a**)



(**b**)

Figure 8. (**a**) Optimization results for 7 kW charging station under Charging Mode 2 and (**b**) optimization results for 11 kW charging station under Charging Mode 2.

4.4. Discussion

The results in Section 4.2 show that the optimization results of transferable loads fluctuate significantly throughout the year, with the fluctuation ranging from 2.08% to 75.09% on 6 January and 18 June, respectively. By comparing the building power load, electricity prices, and electricity carbon emission factors on these two days, the following conclusions can be drawn:

The optimization effect of transferable loads is mainly determined by the occurrence time of the loads, the electricity price, and the fluctuation characteristics of the electricity carbon emission curve. Since a consistent daily schedule is used in building energy consumption simulations, the time distribution of transferable loads is consistent throughout the year for the RSB, with most transferable load consumption occurring between 21:00 and 24:00 (Figure 9). According to the electricity price fluctuation curve of 6 January, this time period was on the descending edge, while on 18 June, it was at the peak. According to the electricity carbon emission fluctuation curves of 6 January and 18 June, this time period was at the peak, but the amplitude of the fluctuation curve on 18 June was significantly higher than that of 6 January. For these reasons, the optimization results on 18 June were significantly better than those on 6 January (Figure 10). Additionally, a "negative electricity price" situation occurred on 18 June, further enhancing the effect of electricity optimization transfer on that day.

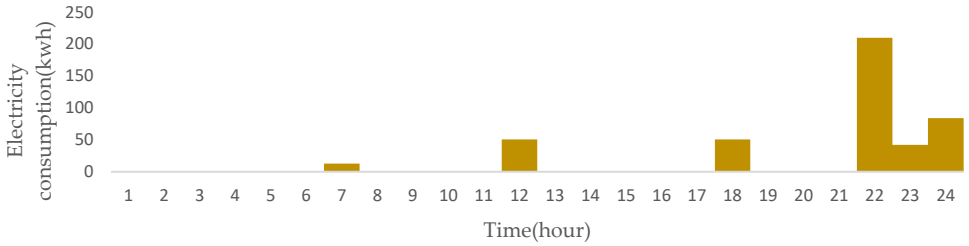


Figure 9. Transferable load distribution.

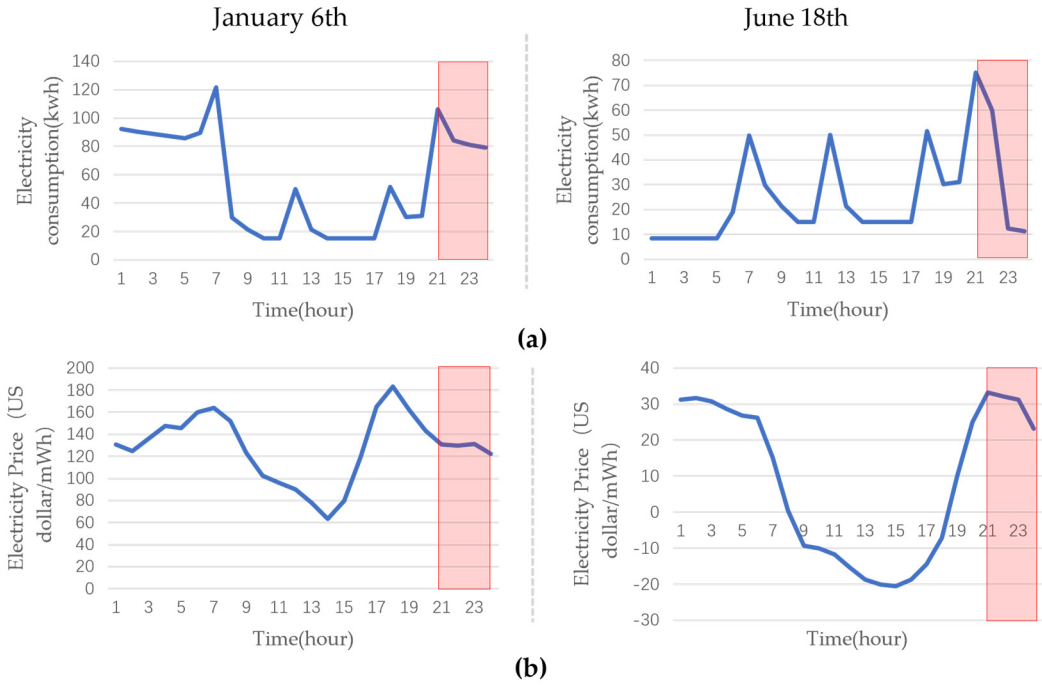


Figure 10. *Cont.*

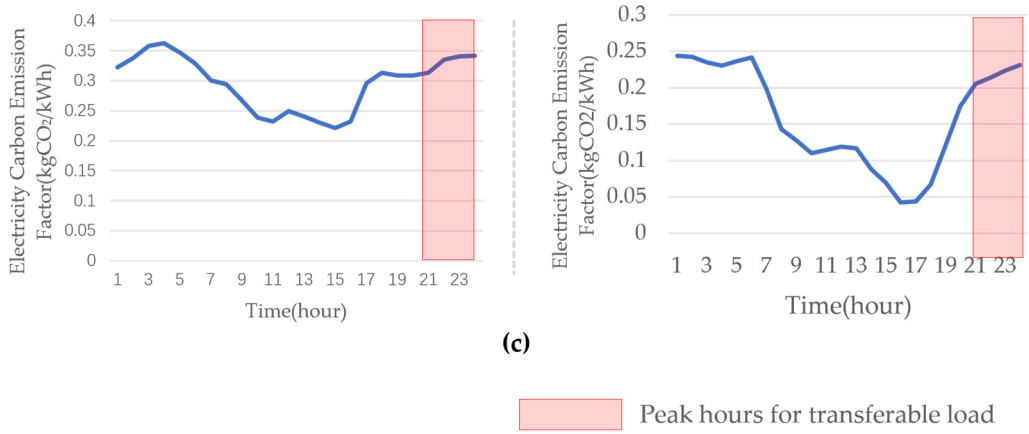


Figure 10. (**a**) Building electricity consumption. (**b**) Electricity price variation curve. (**c**) Electricity carbon emission factor variation curve.

The optimization effect of shifting EV charging load is not only related to the fluctuation characteristics of electricity prices and power carbon emission curves but also to the duration of each charging session. Shorter charging times mean longer schedulable times. Figure 11 shows the daily transfer optimization effect of the comprehensive cost of a single charge at different charging times. The shorter the EV charging time, the better the transfer optimization effect, which is consistent with the optimization results in Section 4.3.

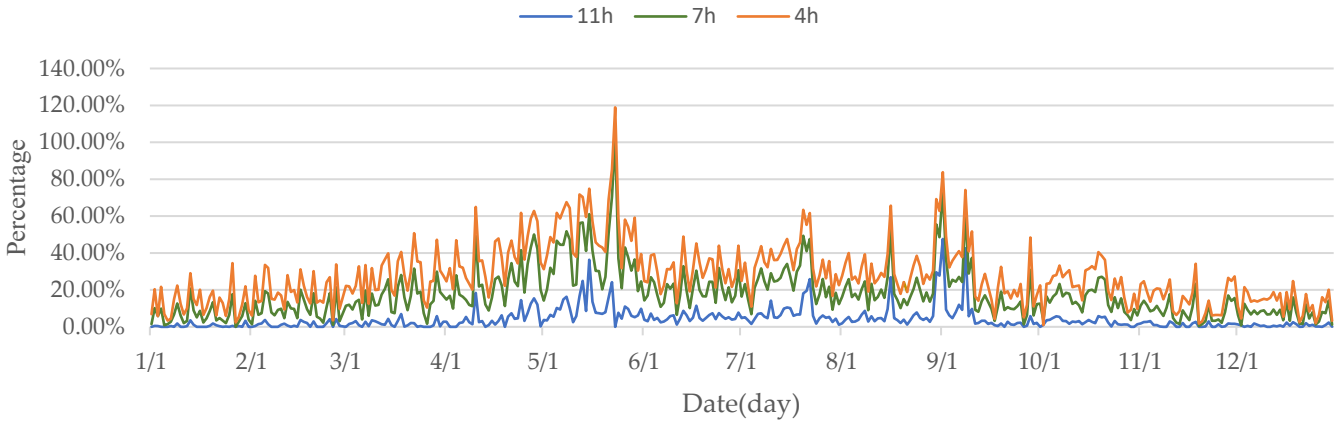


Figure 11. Optimization effects of EV transfer with different charging durations.

5. Conclusions

The integration of renewable energy has resulted in more volatile smart grids, which has introduced new challenges for demand-side management. Nevertheless, the development of smart building technology has made it possible to manage the electricity demand of buildings with a greater degree of adaptability on the demand side. This study establishes a CADR model for typical electrical devices in an RSB. In terms of demand-side management, it is important to consider the carbon emission intensity of power and electricity prices. The model manages the distribution of specific appliance loads, resulting in a substantial reduction in electricity costs, while simultaneously maintaining the same overall power consumption. The case simulation results suggest that the annual comprehensive cost of transferable burdens in the building is reduced by 21.95%. The cost-saving potential of domestic electric vehicles (EVs) was also evaluated under a variety of charging mechanisms. The optimization simulations under two distinct EV charging modes indicate that a high-frequency charging method is more conducive to saving overall electricity costs. It is recommended that users start charging when the battery is in a partially discharged state.

We present a model for optimizing electricity scheduling that is based on typical device types and electricity consumption behaviors. This model simultaneously addresses carbon emissions and electricity prices. Nevertheless, there are some limitations when applying the optimization model and the research results. The implementation of the CADR model must rely on mature intelligent devices such as AMI devices, smart meters, and appliance intelligent controllers, which now lack the necessary conditions for large-scale implementation in the real world. However, such advanced communication intelligent devices are under gradual deployment, which provides the practical possibility for the proposed method and is expected to be widely used shortly. In the future, the proposed CADR model can be tested in real scenarios and continuously improved by cooperating with RSB users. In addition, the CADR model optimization framework in this paper is established based on the standard energy consumption behaviors in residential buildings, which adopts the consistent appliance operation schedule during the whole year, and the EV is also set to charge on regular dates. In real life, the energy consumption behaviors of representative appliances may exhibit significant differences due to the household structure, working schedule, and living habits. It is possible to explore feasible machine learning methods to provide customized CADR models based on the real occupant's energy consumption behaviors in the future. The CADR model in this study only considers the shiftable loads without considering the adjustability of HVAC systems. It is possible to extend the optimization objective of the CADR model in the future by considering the HVAC systems in the optimization equipment to improve the generalization ability of the CADR model.

Author Contributions: Conceptualization, J.Z. and J.R.; methodology, J.Z. and J.R.; software, J.Z.; validation, J.Z. and S.L.; writing—original draft preparation, J.Z.; writing—review and editing, J.Z., L.O. and S.L.; supervision, S.T. All authors have read and agreed to the published version of the manuscript.

Funding: This research was funded by the Science and Technology Project of Jiangxi Province Education Department, grant number GJJ211045.

Data Availability Statement: The datasets used and/or analyzed during the current study are available from the corresponding author upon reasonable request.

Conflicts of Interest: The authors declare that they have no conflicts of interest.

References

1. International Energy Agency. *World Energy Outlook 2023*; IEA: Paris, France, 2023; p. 278.
2. Ruan, J.; Xu, Z.; Su, H. Towards interdisciplinary integration of electrical engineering and earth science. *Nat. Rev. Electr. Eng.* **2024**, *1*, 278–279. [CrossRef]
3. Wang, B.; Zhang, C.; Dong, Z.Y. Interval Optimization Based Coordination of Demand Response and Battery Energy Storage System Considering SOC Management in a Microgrid. *IEEE Trans. Sustain. Energy* **2020**, *11*, 2922–2931. [CrossRef]
4. Ding, Y.; Sun, X.; Ruan, J.; Shi, W.; Wu, H.; Xu, Z. Customized decentralized autonomous organization based optimal energy management for smart buildings. *Appl. Energy* **2023**, *376*, 124223. [CrossRef]
5. Ruan, J.; Liang, G.; Zhao, H.; Liu, G.; Sun, X.; Qiu, J.; Xu, Z.; Wen, F.; Dong, Z.Y. Applying Large Language Models to Power Systems: Potential Security Threats. *IEEE Trans. Smart Grid* **2024**, *14*, 4035–4046. [CrossRef]
6. Broeer, T.; Fuller, J.; Tuffner, F.; Chassin, D.; Djilali, N. Modeling framework and validation of a smart grid and demand response system for wind power integration. *Appl. Energy* **2014**, *113*, 199–207. [CrossRef]
7. Drury, E.; De Coninck, G.; D'Haeseleer, W. Demand response flexibility and flexibility potential of residential smart appliances: Experiences from large pilot test in Belgium. *Energy Build.* **2015**, *107*, 264–275.
8. Lu, N. An evaluation of the HVAC load potential for providing load balancing service. *IEEE Trans. Smart Grid* **2012**, *3*, 50–64. [CrossRef]
9. Shayestegan, M.; Abunima, H.; Salim Reza, M.; Akhtaruzzaman, M.; Alamoud, A.; Sopian, K.; Amin, N. An intelligent system architecture in home energy management systems (HEMS) for efficient demand response in smart grid. *Energy Build.* **2017**, *138*, 252–263.
10. Azar, A.G.; Jacobsen, R.H. Appliance Scheduling Optimization for Demand Response. *Intell. Syst.* **2016**, *9*, 50–64.
11. Klein, L.; Kwak, J.Y.; Kavulya, G.; Jazizadeh, F.; Becerik-Gerber, B.; Varakantham, P.; Tambe, M. Coordinating occupant behavior for building energy and comfort management using multi-agent systems. *Autom. Constr.* **2012**, *22*, 525–536. [CrossRef]

12. Bianchini, G.; Casini, M.; Vicino, A.; Zarrilli, D. Demand-response in building heating systems: A Model Predictive Control approach. *Appl. Energy* **2016**, *168*, 159–170. [CrossRef]
13. Hong, T.; Taylor-Lange, S.C.; Oca, S.D.; Yan, D.; Corgnati, S.P. Advances in research and applications of energy-related occupant behavior in buildings. *Energy Build.* **2016**, *116*, 694–702. [CrossRef]
14. Sehar, F.; Pipattanasomporn, M.; Rahman, S. An energy management model to study energy and peak power savings from PV and storage in demand responsive buildings. *Appl. Energy* **2016**, *173*, 406–417. [CrossRef]
15. Dolatabadi, M.K.; Dolatabadi, A. Optimal electrical and thermal energy management of a residential energy hub, integrating demand response and energy storage system. *Energy Build.* **2015**, *87*, 517–530.
16. Babonneau, F.; Caramanis, M.; Haurie, A. A linear programming model for power distribution with demand response and variable renewable energy. *Appl. Energy* **2016**, *181*, 83–95. [CrossRef]
17. Ali, M.; Jokisalo, J.; Siren, K.; Lehtonen, M. Combining the Demand Response of direct electric space heating and partial thermal storage using LP optimization. *Electr. Power Syst. Res.* **2014**, *106*, 160–167. [CrossRef]
18. Neves, D.; Silva, C.A. Optimal electricity dispatch on isolated mini-grids using a demand response strategy for thermal storage backup with genetic algorithms. *Energy* **2015**, *82*, 436–445. [CrossRef]
19. Hu, M.; Xiao, F. Price-responsive model-based optimal demand response control of inverter air conditioners using genetic algorithm. *Appl. Energy* **2018**, *219*, 151–164. [CrossRef]
20. Lauro, F.; Moretti, F.; Capozzoli, A.; Panzieri, S. Model predictive control for building active demand response systems. *Energy Procedia* **2015**, *83*, 494–503. [CrossRef]
21. Hedegaard, R.E.; Pedersen, T.H.; Petersen, S. Multi-market demand response using economic model predictive control of space heating in residential buildings. *Energy Build.* **2017**, *150*, 253–261. [CrossRef]
22. Ruan, J.; Liang, G.; Zhao, J.; Zhao, H.; Qiu, J.; Wen, F.; Dong, Z.Y. Deep learning for cybersecurity in smart grids: Review and perspectives. *Energy Convers. Econ.* **2023**, *4*, 233–251. [CrossRef]
23. Yu, R.; Yang, W.; Rahardja, S. A statistical demand-price model with its application in optimal real-time price. *IEEE Trans. Smart Grid* **2012**, *3*, 1734–1742. [CrossRef]
24. Nakabi, T.A.; Toivanen, P. An ANN-based model for learning individual customer behavior in response to electricity prices. *Sustain. Energy Grids Netw.* **2019**, *18*, 100212. [CrossRef]
25. Ruan, J.; Liu, G.; Qiu, J.; Liang, G.; Zhao, J.; He, B.; Wen, F. Time-varying price elasticity of demand estimation for demand-side smart dynamic pricing. *Appl. Energy* **2022**, *322*, 119520. [CrossRef]
26. Andruszkiewicz, J.; Lorenc, J.; Weychan, A. Seasonal variability of price elasticity of demand of households using zonal tariffs and its impact on hourly load of the power system. *Energy* **2020**, *196*, 117175. [CrossRef]
27. Ruan, J.; Liang, G.; Zhao, J.; Lei, S.; He, B.; Qiu, J.; Dong, Z.Y. Graph Deep-Learning-Based Retail Dynamic Pricing for Demand Response. *IEEE Trans. Smart Grid* **2023**, *14*, 4385–4397. [CrossRef]
28. Parrish, B.; Heptonstall, P.; Gross, R.; Sovacool, B.K. A systematic review of motivations, enablers and barriers for consumer engagement with residential demand response. *Energy Policy* **2020**, *138*, 111221. [CrossRef]
29. Zhou, B.; Li, W.; Chan, K.W.; Cao, Y.; Kuang, Y.; Liu, X.; Wang, X. Smart home energy management systems: Concept, configurations, and scheduling strategies. *Renew. Sustain. Energy Rev.* **2016**, *61*, 30–40. [CrossRef]
30. National Bureau of Statistics of China. *China Statistical Year-Book 2023*; China Statistics Press: Beijing, China, 2023; p. 185.
31. *GB55015-2021*; General Code for Energy Efficiency and Renewable Energy Application in Buildings. Ministry of Housing and Urban-Rural Development of the People's Republic of China (China Statistics Press): Beijing, China, 2021; pp. 69–75.
32. The State Council of the People's Republic of China. *New Energy Vehicle Industry Development Plan (2021–2035)*; The State Council of the People's Republic of China: Beijing, China, 2020.
33. Jin, L.; Wang, S.; He, H. *International Council on Clean Transportation. Real-World Performance of Battery Electric Passenger Cars in China: Energy Consumption, Range, and Charging Patterns*; International Council on Clean Transportation: Washington, DC, USA, 2023.
34. Zhou, L.; Gao, Y.; Shi1, B.Y. *Vehicle Mileage Insight Report 2023*; Yiche Research Institute: Hangzhou, China, 2023.
35. *DG/TJ08-7-2021*; Standards for Design of Traffic and Setting up Parking Garages (Lots) in Architectural Engineering. Shanghai Municipal Commission of Housing and Urban-Rural Development. Tongji University Press: Shanghai, China, 2021; pp. 69–75.
36. Report on the Work of the Government 2023. Available online: https://www.shanghai.gov.cn/2023nzfgzbg/index.html (accessed on 25 October 2024).

Disclaimer/Publisher's Note: The statements, opinions and data contained in all publications are solely those of the individual author(s) and contributor(s) and not of MDPI and/or the editor(s). MDPI and/or the editor(s) disclaim responsibility for any injury to people or property resulting from any ideas, methods, instructions or products referred to in the content.